

Implications of a VLBI Distance to the Double Pulsar J0737–3039A/B

A.T. Deller^{1*}, M. Bailes¹, S.J. Tingay²

¹Centre for Astrophysics and Supercomputing

Swinburne University of Technology

Mail H39, P.O. Box 218, Hawthorn, VIC 3122, Australia

²Curtin Institute of Radio Astronomy

Curtin University of Technology, Bentley, WA, Australia

*To whom correspondence should be addressed. E-mail: adeller@astro.swin.edu.au.

The double pulsar J0737–3039A/B is a unique system with which to test gravitational theories in the strong–field regime. However, the accuracy of such tests will be limited by knowledge of the distance and relative motion of the system. Here we present very long baseline interferometry observations which reveal that the distance to PSR J0737–3039A/B is 1150^{+220}_{-160} pc, more than double previous estimates, and confirm its low transverse velocity (~ 9 km s^{−1}). Combined with a decade of pulsar timing, these results will allow tests of gravitational radiation emission theories at the 0.01% level, putting stringent constraints on theories which predict dipolar gravitational radiation. They also allow insight into the system’s formation and the source of its high–energy emission.

The double pulsar system J0737–3039A/B (1, 2) is one of eight known double neutron star (DNS) systems, and the only system in which both neutron stars are visible as pulsars. The

‘A’ pulsar, which has been spun-up by accretion (“recycled”) to a period $P = 22.7$ ms, was discovered first; the non-recycled ‘B’ pulsar ($P = 2.77$ s) was found during follow-up timing observations. PSR J0737–3039A/B is the most relativistic known DNS system. It has an orbital period of 2.5 hours and a coalescence time (due to orbital energy loss to gravitational radiation) of 85 Myr. Compared to most DNS systems, it has a low eccentricity (0.08) and is thought to possess a low transverse velocity [10 km s^{-1} ; (3)], which is difficult to explain in standard models of pulsar formation. Pulsar timing of PSR J0737–3039A/B produces results consistent with the theory of general relativity (GR) at the 0.05% level (3).

The distance to PSR J0737–3039A/B is estimated using the pulsar dispersion measure (DM) and models of the ionized component of the Galaxy (4, 5). However, distances derived in this manner have been shown to be in error by a factor of two or more for individual systems [e.g. PSR B0656+14; (6)]. A more accurate distance to the PSR J0737–3039A/B system is needed in order to determine the contribution of kinematic effects to pulsar timing, whose uncertainty would otherwise limit the precision GR tests could achieve; to establish the source of the x-ray emission from the system (7, 8); and to refine the estimated radio luminosity.

We used the Australian Long Baseline Array (LBA) to obtain a model-independent distance to PSR J0737–3039A/B, through the direct measurement of its annual geometric parallax. We have made seven very long baseline interferometry (VLBI) observations of PSR J0737–3039A/B over an 18 month period between August 2006 and February 2008, which allowed us to fit the system’s position, proper motion and parallax [for more details see (9), Table 1 and Fig. 1; all errors are 1σ unless otherwise stated].

The distance to PSR J0737–3039A/B is 1150_{-160}^{+220} pc, which is inconsistent with previous DM-based estimates of 570 pc (4) and 480 pc (5). Our measurement is more significant than the distance of 333_{-133}^{+667} pc obtained through a marginal timing parallax detection (3), which differed by approximately 1σ from our result. The revised value of electron density along the

line of sight to PSR J0737–3039A/B is 0.043 cm^{-3} , suggesting that the influence of the Gum nebula (a large, ionized hydrogen region between the Earth and PSR J0737–3039A/B) along this line of sight is less than originally thought. The proper motion of PSR J0737–3039A/B is $4.37 \pm 0.65 \text{ mas yr}^{-1}$, consistent with a previous timing measurement of $4.2 \pm 0.6 \text{ mas yr}^{-1}$ (3).

We used the revised distance to PSR J0737–3039A/B to estimate the precision attainable for testing predictions of gravitational wave emission from the system. In order to compare the rate of change of orbital period (\dot{P}_b) due to the loss of energy to gravitational radiation with the GR prediction, the observed \dot{P}_b must be measured as accurately as possible [the current significance is 70σ (3)], and contributing factors to \dot{P}_b other than GR must be estimated and subtracted as accurately as possible. For PSR J0737–3039A/B, the major contributing factors are differential Galactic rotation (\dot{P}_b^{rot}), acceleration towards the plane of the Galaxy (\dot{P}_b^z), and the apparent acceleration caused by the transverse motion of the system [the Shklovskii effect \dot{P}_b^{Shk} ; (10)], to which we will refer collectively as galactic and kinematic contributions (\dot{P}_b^{gk}). For the newly-calculated distance of 1150 pc, the magnitude of these effects is calculated using Equations 2.12 and 2.28 from (11) as:

$$\frac{\dot{P}_b^{\text{rot}}}{P_b} = -\frac{v_0^2}{c R_0} \times \left(\cos l + \frac{\beta}{\sin^2 l + \beta^2} \right) \quad (1)$$

$$\frac{\dot{P}_b^z}{P_b} = -\frac{K_z}{c} \sin b \quad (2)$$

$$\frac{\dot{P}_b^{\text{Shk}}}{P_b} = \frac{\mu^2 d}{c} \quad (3)$$

where l , b and z are galactic longitude, latitude and height respectively, d and μ are pulsar distance and proper motion, R_0 and v_0 are the Galactic radius and speed of the Solar System [taken to be 7.5 kpc and 195 km s^{-1} respectively (12)], K_z is the vertical gravitational potential of the Galaxy [taken from (13) as $0.45 \text{ km}^2 \text{ s}^{-2} \text{ pc}^{-1}$ at the height of PSR J0737–3039A/B] and c is the speed of light. The dominant uncertainties are in d (16%), μ (15%), and R_0 , v_0 and K_z ,

whose errors are estimated at $\sim 10\%$.

Equations (1)-(3) give $\dot{P}_b^{\text{rot}}/P_b = (-4.3 \pm 0.7) \times 10^{-20} \text{ s}^{-1}$, $\dot{P}_b^z/P_b = (3.8 \pm 0.8) \times 10^{-21} \text{ s}^{-1}$, and $\dot{P}_b^{\text{Shk}}/P_b = (5.3 \pm 1.8) \times 10^{-20} \text{ s}^{-1}$. Combining these terms gives $\dot{P}_b^{\text{gk}}/P_b = (1.5 \pm 2.1) \times 10^{-20} \text{ s}^{-1}$, and multiplying by the observed orbital period $P_b = 8834.5 \text{ s}$ (3) yields the net effect of these terms on the observed orbital period derivative: $\dot{P}_b^{\text{gk}} = (1.3 \pm 1.8) \times 10^{-16}$.

These contributions to the orbital period derivative are four orders of magnitude below the GR contribution, and two orders of magnitude below the current measurement error [$\dot{P}_b^{\text{obs}} = (-1.252 \pm 0.017) \times 10^{-12}$; (3)]. Thus, with the current accuracy in the measurement of distance and transverse velocity, GR tests can be made to the 0.01% level with PSR J0737–3039A/B using \dot{P}_b . However, about ten years of further precision timing will be required to reach this point. Measuring \dot{P}_b at this level will place stringent requirements on the class of gravitational theories which predict significant amounts of dipolar gravitational radiation, exceeding the best Solar System tests (3). Measuring the moment of inertia of pulsar A, however, would require another order of magnitude improvement in the measurement precision of \dot{P}_b (3). In the near future, additional VLBI and/or timing measurements can be expected to reduce the error in both the distance and velocity of PSR J0737–3039A/B below 10%; however, even with negligible error in these parameters, the existing accuracy of measurements of R_0 , v_0 and K_z would limit the accuracy of \dot{P}_b measurements in this system to 0.004%. To attain the 10^{-5} precision necessary to measure the neutron star moment of inertia, the constants R_0 and v_0 must be measured to a precision approaching 1%.

X-ray observations of PSR J0737–3039A/B show that most of the x-ray emission from the system is modulated at the spin period of the A pulsar (7, 14, 8, 15), but there has been considerable debate over where and how the x-rays are generated. Normally, pulsar x-ray emission is thought to have a magnetospheric or thermal origin (16). However, the small binary separation and interaction of the pulsar wind of the A pulsar with the magnetosphere of the B

pulsar (17) provides alternate x-ray generation mechanisms.

The spin-down luminosity of pulsar A is over three orders of magnitude greater than that of pulsar B. Thus, pulsar A is likely to dominate any magnetospheric x-ray emission from the system. Whilst a wholly magnetospheric (power-law) origin for the observed x-ray emission is plausible, the neutral hydrogen column density [$N_{\text{H}} \sim 1.5 \times 10^{21} \text{ cm}^{-2}$; (8)] implied by the model is higher than expected from the pulsar's previously assumed location in the Gum nebula. The Gum nebula is believed to be approximately 500 pc distant, with a depth of several hundred pc (5).

However, the value of N_{H} is consistent with the usual average of 10 neutral hydrogen atoms for every free electron along the line of sight. Our revised distance estimate places PSR J0737–3039A/B beyond the Gum nebula, implying that the measured value for N_{H} is not discrepant. It also increases the estimated x-ray luminosity by a factor of 5, but the revised value for a power-law fit ($1.2 \times 10^{31} \text{ erg s}^{-1}$) remains consistent with known relations between pulsar spin-down luminosity and x-ray luminosity (18). Hence, our result supports a power-law model of magnetospheric origin (from pulsar A) for the bulk of the x-ray emission from PSR J0737–3039A/B.

The discovery of PSR J0737–3039A led to a marked upward revision in the estimated Galactic merger rate of DNS systems (19), although uncertainty over the characteristics of recycled pulsars means that the true value of the merger rate remains poorly constrained. Specifically, the distribution of recycled pulsar luminosities is generally extrapolated from the entire pulsar population (19) even though it (along with the distributions of pulse shape and beaming fraction) appears to differ from the distribution for slower pulsars (20). Our revised distance shows that the radio luminosity of PSR J0737–3039A is a factor of five greater than previously assumed. If this revision were to markedly influence the recycled pulsar luminosity function, then the assumed space density of DNS systems would be reduced, with a corresponding impact on

DNS merger rates estimations.

Finally, we used the measured transverse velocity for PSR J0737–3039A/B (24_{-6}^{+9} km s⁻¹) to constrain models of the formation of the system. After subtracting estimates of the peculiar motion of the Solar System and Galactic rotation (21), we measure a transverse velocity in local standard of rest of 9_{-3}^{+6} km s⁻¹. This is comparable to the unadjusted value of 10 km s⁻¹ presented in (3), and is within the range of transverse velocities expected for the massive stars which are DNS progenitors [~ 20 km s⁻¹; (22)]. Because the transverse velocity of PSR J0737–3039A/B is so low, if the system received a large velocity kick at birth, it must have a large radial velocity. However, there are no observational methods available to determine the radial velocity in a DNS system.

Because of the accurate measurement of its Shapiro delay, PSR J0737–3039A/B is known to lie edge-on (3). If the only kick it received was provided by the loss of binding energy during the supernova explosion, the resultant 3D space velocity should be on the order of ~ 50 km s⁻¹, estimated from the system’s observed eccentricity and orbital velocity (23). This space velocity would be constrained to the plane of the orbit. From simple geometry, the probability of observing a transverse velocity less than 10 km s⁻¹ is about one in eight, which is small, but not unreasonable. Conversely, if the double pulsar had received a large kick (24), the odds of observing such a low transverse velocity become increasingly remote. Not only would the radial velocity have to be increasingly large, but the inclination angle of the system must not be altered by the kick. Hence, our transverse velocity results reinforce those of (3) and are consistent with the interpretation of (25), who argue for almost no mass loss and kick in the case of PSR J0737–3039A/B.

The implication of low kick velocities in PSR J0737–3039A/B–like systems offers a possible, albeit speculative, explanation to the formation of PSR J1903+0327, a heavy, highly recycled millisecond pulsar (mass 1.8 solar masses, period 2.15 ms) with a main sequence com-

panion of one solar mass (26). The orbit of such a pulsar should have been highly circularized during the mass-transfer phase (27). However, PSR J1903+0327 possesses an intermediate orbital eccentricity ($e = 0.44$).

A formation mechanism for PSR J1903+0327 has been suggested in which a triple system experiences a white dwarf-neutron star coalescence (28). However, a coalescing DNS system such as PSR J0737–3039A/B could also create a PSR J1903+0327-like pulsar. Thus, given the low velocity of PSR J0737–3039A/B, an alternative formation mechanism for PSR J1903+0327 involves a triple system containing a close DNS binary and a main sequence star.

References and Notes

1. M. Burgay, *et al.*, *Nature* **426**, 531 (2003).
2. A. G. Lyne, *et al.*, *Science* **303**, 1153 (2004).
3. M. Kramer, *et al.*, *Science* **314**, 97 (2006).
4. J. H. Taylor, J. M. Cordes, *ApJ* **411**, 674 (1993).
5. J. M. Cordes, T. J. W. Lazio, *ArXiv e-prints* **0207156** (2002).
6. W. F. Brisken, S. E. Thorsett, A. Golden, W. M. Goss, *ApJ* **593**, L89 (2003).
7. M. A. McLaughlin, *et al.*, *ApJ* **605**, L41 (2004).
8. A. Possenti, *et al.*, *ApJ* **680**, 654 (2008).
9. Information on materials and methods is available on science online.
10. I. S. Shklovskii, *Soviet Astronomy* **13**, 562 (1970).
11. T. Damour, J. H. Taylor, *ApJ* **366**, 501 (1991).

12. W. S. Dias, J. R. D. Lépine, *ApJ* **629**, 825 (2005).
13. J. Holmberg, C. Flynn, *MNRAS* **352**, 440 (2004).
14. S. Chatterjee, B. M. Gaensler, A. Melatos, W. F. Brisken, B. W. Stappers, *ApJ* **670**, 1301 (2007).
15. A. Pellizzoni, A. Tiengo, A. De Luca, P. Esposito, S. Mereghetti, *ApJ* **679**, 664 (2008).
16. W. Becker, *Highly Energetic Physical Processes and Mechanisms for Emission from Astrophysical Plasmas*, P. C. H. Martens, S. Tsuruta, M. A. Weber, eds. (2000), vol. 195 of *IAU Symposium*, p. 49.
17. M. Lyutikov, *MNRAS* **353**, 1095 (2004).
18. J. E. Grindlay, *et al.*, *ApJ* **581**, 470 (2002).
19. V. Kalogera, *et al.*, *ApJ* **601**, L179 (2004).
20. M. Kramer, *et al.*, *ApJ* **501**, 270 (1998).
21. F. Mignard, *A&A* **354**, 522 (2000).
22. M. W. Feast, M. Shuttleworth, *MNRAS* **130**, 245 (1965).
23. A. Blaauw, *Bull. Astron. Inst. Netherlands* **15**, 265 (1961).
24. B. Willems, J. Kaplan, T. Fragos, V. Kalogera, K. Belczynski, *Phys. Rev. D* **74**, 043003 (2006).
25. T. Piran, N. J. Shaviv, *Physical Review Letters* **94**, 051102 (2005).
26. D. J. Champion, *et al.*, *Science* **320**, 1309 (2008).

27. M. A. Alpar, A. F. Cheng, M. A. Ruderman, J. Shaham, *Nature* **300**, 728 (1982).

28. E. P. J. van den Heuvel, *Science* (2008).

29. The authors acknowledge discussions with M. Kramer and E. van den Heuvel. ATD is supported via a Swinburne University of Technology Chancellor's Research Scholarship and a CSIRO postgraduate scholarship. The Long Baseline Array is part of the Australia Telescope which is funded by the Commonwealth of Australia for operation as a National Facility managed by CSIRO.

Table 1. Fitted VLBI results for PSR J0737–3039A/B

Parameter	Value
Right Ascension α (RA; J2000) ¹	07:37:51.248419(26)
Declination δ (Dec; J2000) ¹	−30:39:40.71431(10)
Proper motion in RA ($\mu_\alpha \times \cos \delta$; mas yr ^{−1})	−3.82(62)
Proper motion in Declination (μ_δ ; mas yr ^{−1})	2.13(23)
Parallax (mas)	0.87(14)
Distance (pc)	1150 ⁺²²⁰ _{−160}
Transverse velocity (km s ^{−1})	24 ⁺⁹ _{−6}
Transverse velocity in LSR ² (km s ^{−1})	9 ⁺⁶ _{−3}
Reference epoch (MJD)	54100

¹As discussed in (9), the actual error in the pulsar position is dominated by the alignment of the barycentric reference frame used for pulsar timing and the quasi-inertial frame used for VLBI, and is approximately an order of magnitude greater than the formal fit error shown here

²Local Standard of Rest

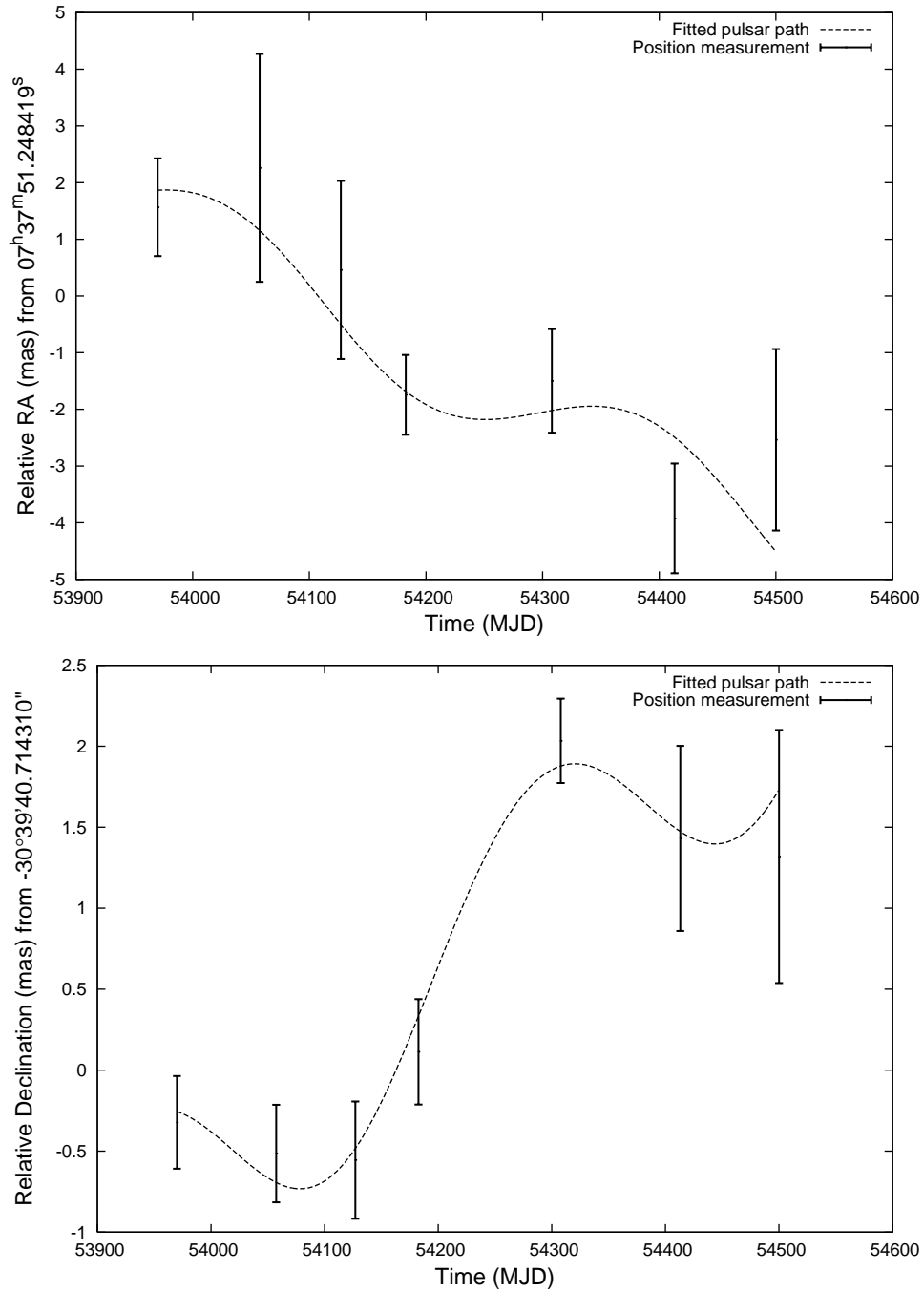


Fig. 1: Motion of PSR J0737–3039A/B plotted against time. **(Top)** Offset in right ascension; **(Bottom)** Offset in declination. The best fit (dashed line) is overlaid on the measured positions. The reduced chi-squared of the fit was 0.79, implying that the measurement errors (and thus the errors on fitted parameters) might be overestimated and hence conservative.

Supporting Online Material

Materials and Methods

Details of the observational, correlation, and post-processing strategies used are covered in detail in (*S1*) and are summarized here. Seven observational epochs spanned an 18 month period from August 2006 to February 2008. Approximately six hours of on-source time (divided equally between the phase reference calibrator B0736–303 and PSR J0737–3039A/B) were available per epoch, and all available antennas from the Australian Long Baseline Array (LBA) were utilized. The LBA is a network of six radio telescopes which provides the best means for VLBI study of southern radio sources. Of these, five telescopes are equipped to make observations at 1650 MHz, which was the observing frequency utilized. These were the three ATNF antennas (ATCA, Parkes, Mopra), the University of Tasmania antenna near Hobart and, when available, the 70m NASA Deep Space Network (DSN) antenna at the Tidbinbilla station. In each session, the on-source time was spread over the ten hour period that PSR J0737–3039A/B was visible to the array in order to obtain good *uv* coverage. Four 16 MHz bands were used, quantized at two bit precision to give a total data rate of 256 Mbps.

The phase reference calibrator B0736–303 is a bright and predominantly compact radio source separated by ~ 20 arcminutes from PSR J0737–3039A/B. Since the position of B0736–303 was not known precisely in the International Celestial Reference Frame (ICRF) at the outset of this project, its position was determined by aligning the obtained position for PSR J0737–3039A/B with the value known from timing (*S2*), accounting for the pulsar proper motion. This is possible due to the alignment at the milliarcsecond level of the ICRF with the barycentric reference frame used for pulsar timing. The final positional accuracy for B0736–303 was estimated to be better than 5 milliarcseconds, which is acceptable for the short calibrator throw (20 arcminutes) used here. This use of the timing position of PSR J0737–3039A/B to obtain the

calibrator position means that the VLBI observations do not contribute to an improvement in the reference position for PSR J0737–3039A/B, as the error in the ultimately obtained position is dominated by the uncertainty in alignment between the ICRF and barycentric reference frames [1-2 milliarcseconds; (*S3*)]. A six minute target/calibrator cycle was employed, with observing time divided equally between the target and calibrator.

The data were correlated, using matched filtering (gating) on pulse profiles, with the DiFX software correlator (*S4*). Pulse profile filtering improves the signal to noise when observing a periodic signal by weighting the correlator output according to the varying pulsar flux. For PSR J0737–3039A/B, the pulse filter was set based on the signal from pulsar A only, since this dominates the emission in the system. The pulse filtering yields a factor of 2.5 improvement in the observed signal to noise ratio. The most accurate published pulsar ephemeris (*S2*) was used to set the pulse filter. The visibility data for each epoch was weighted by baseline sensitivity and imaged using natural weighting.

The data were fitted using an iterative approach designed to estimate and account for systematic errors, described in detail in (*S1*). This approach generated a position and position error for each 16 MHz band at each epoch, and the single-band positions were used to obtain a single weighted centroid position for each epoch. Estimates of systematic error at each epoch were made by inspecting the reduced chi-squared of the fit to position centroid, and these estimates were added in quadrature to the centroid position error. The final seven position measurements were then fit for position, proper motion and parallax using the iterative minimization code described in (*S1*). The reduced chi-squared of the final fit was 0.79, indicating that the quoted errors for the fitted values may be slightly conservative.

SOM References and Notes

S1. A. T. Deller, S. J. Tingay, W. F. Brisken, *ApJ* **690**, 198 (2009).

S2. M. Kramer, *et al.*, *Science* **314**, 97 (2006).

S3. A. T. Deller, J. P. W. Verbiest, S. J. Tingay, M. Bailes, *ApJL* **685**, L67 (2008).

S4. A. T. Deller, S. J. Tingay, M. Bailes, C. West, *PASP* **119**, 318 (2007).